

Structure of the set of feasible neural commands for complex motor tasks

Cohn BA¹, Szedlák M², Fukuda K², Valero-Cuevas FJ¹, and Gärtner B²

Abstract—The brain must select its control strategies among an infinite set of possibilities, thereby researchers believe that it must be solving an optimization problem. While this set of feasible solutions is infinite and lies in high dimensions, it is bounded by kinematic, neuromuscular, and anatomical constraints, within which the brain must select optimal solutions. That is, the set of feasible activations is well structured. However, to date there is no method to describe and quantify the structure of these high-dimensional solution spaces, other than bounding boxes or dimensionality reduction algorithms that do not capture its full structure. We present a novel approach based on the well-known Hit-and-Run algorithm in computational geometry to extract the structure of the feasible activations that produce 50% of maximal fingertip force. We use a realistic model of a human index finger with 7 muscles, 4DOF, and 4 output dimensions. For a given force vector at the endpoint, the feasible activation space is a 3D convex polytope, embedded in the 7D unit cube. It is known that explicitly computing the volume of this polytope can become too computationally complex in many instances. However, our algorithm was able to produce 1,000,000 random points in the feasible activation space, which converged to the uniform distribution. The computed distribution of activation across each muscle shed light onto the structure of these solution spaces—rather than simply exploring their maximal and minimal values. Although this paper presents a 7 dimensional case of the index finger, our methods extend to systems with up to at least 40 muscles. This will allow our motor control community to understand the distributions of feasible muscle activations, which will provide important contextual information into the learning, optimization and adaptation of motor patterns in future research.

I. INTRODUCTION

Muscle redundancy is the term used to describe the underdetermined nature of neural control of musculature. The classical notion of muscle redundancy proposes that, faced with an infinite number of possible muscle activation patterns for a given task, the nervous system optimizes in some fashion to select one solution. Here, each of N muscles represents a dimension of control on an end effector, and at any moment of a task, a muscle activation pattern exists as a point in \mathbb{R}^N , with a level of activation for every muscle involved [18]. Thus researchers often seek to infer the optimization approach and the cost functions the nervous system utilizes to select effective points in activation space to produce natural behavior [2], [12], [13], [16], [4], [7].

*This work was supported by NIH NIAMS R01AR050520 and R01AR052345 grants, and SNF Project 200021-150055-1.

¹Departments of Biomedical Engineering and Computer Science at the University of Southern California Viterbi School of Engineering, Los Angeles, CA 90089, USA brianaco@usc.edu

²Department of Computer Science, ETH Zurich, Switzerland

Implicit in these optimization procedures is the notion that there exists a well structured set of feasible solutions. Thus several of us have focused on describing and understanding those high-dimensional subspaces embedded in \mathbb{R}^N [10], [11], [15], [18], [8].

For the case of submaximal and static force production with a limb, the muscle redundancy problem is phrased in computational geometry: find the structure of the set of all feasible muscle activations, given the limb mechanics and the task constraints [1], [18], [17], [8]. We aim to explore what the solution space looks like, and uncover the structure of the feasible activation space for a given static force task. If each muscle's maximal activation is normalized to 1, the constraint $\mathbf{a} \in [0,1]^n$ describes that the feasible activation space lies in the n -dimensional unit cube (also called the n -cube); the activation space for the index finger is within the unit 7-cube.

A. High dimensionality difficulties

Consider a model of a static fingertip force, with 7 muscles articulating the index finger's 4 Degrees of Freedom. Assuming independent control of each muscle (non-synergistic model), each muscle has a unique force vector at the endpoint; the end effector has 7 unique vectors it can linearly combine to generate any vector of static force. This yields a unit 7-cube in charge of producing a 4-dimensional output wrench. On order to uncover the structure and relationship of these spaces, we cannot visualize all dimensions simultaneously as we could with a simple 3-muscle model.

This convex polytope is called the *feasible activation set*. To date, the structure of this high-dimensional polytope is inferred by its bounding box [10], [15], [8]. But the bounding box of a convex polytope will always overestimate its volume, and lose the details of its shape. Empirical dimensionality-reduction methods have also been used to calculate a basis vectors for such subspaces [3], [5], [9]. But those basis vectors only provide a description of the dimension, orientation, and aspect ratio of the polytope, but not of its boundaries or internal structure.

Here we present a novel application of the well-known Hit-and-Run algorithm [14] to describe the internal structure of these high-dimensional feasible activation sets. The input to our hit-and-run procedure requires a task force, along with the system's endpoint Jacobian, maximal tendon forces, and a moment arm matrix.

We applied our approach to two separate musculoskeletal models: 1. A fabricated schematic system, which we

designed to have three muscles articulating one DOF, and one dimension of output force. 2. A realistic model, with seven muscles articulating four DOFs, and four dimensional output force [18]. With this, below are the key ideas and findings we present with this paper:

- For some muscles, we found that the bounding box exceptionally misconstrues the actual shape of the feasible activation space.
- Hit-and-run sampling of the solution space is computationally tractable; fewer than ten thousand points uncovered the shape of the distributions.
- Our approach provides a more granular context to the space within which the central nervous system optimizes.
- We apply six different cost functions (post-hoc) to all solutions, thereby providing spatial context to where 'optimal' solutions lie within the space.
- We designed an interactive parallel coordinates platform for visualizing and manipulating constraints to the solution space, such as muscle dysfunction, muscle hyperactivity, as well as constraining the upper and lower bounds for six different cost functions. We can compare cost functions side-by-side and view subsets of the dataset after applying cost function constraints.

II. METHODS

In the case of a schematic tendon-driven limb with three muscles, the feasible activation space is the unit cube (as muscles can only be activated positively from 0 to a maximal normalized value of 1). As explained in [17], when task constraints are introduced to the system, the feasible activation set is further reduced; in this context, a task is a static force vector produced at the endpoint of the limb, which is represented as a set of inequality constraints. Thus if this simple limb meets all constraints, the feasible activation set of the polytope P contains all feasible activations $\mathbf{a} \in \mathbb{R}^n$ that satisfy

$$\mathbf{f} = \mathbf{A}\mathbf{a}, \mathbf{a} \in [0, 1]^n,$$

where $\mathbf{f} \in \mathbb{R}^m$ is a fixed force vector and $\mathbf{A} = \mathbf{J}^{-T} \mathbf{R} \mathbf{F}_0 \in \mathbb{R}^{m \times n}$ —the matrices of the Jacobian of the limb, the moment arms of the tendons, and the strengths of the muscles, respectively [18], [17]. P is bounded by the unit n -cube since all variables a_i , $i \in [n]$ are bounded by 0 and 1 from below, above respectively. Consider the following 1×3 fabricated example, where the task is a 1N unidimensional force.

$$1 = \frac{10}{3}a_1 - \frac{53}{15}a_2 + 2a_3$$

$$a_1, a_2, a_3 \in [0, 1],$$

the set of feasible activations is given by the shaded set in Figure II.

A. Hit-and-Run algorithm

Hit-and-Run is a method used to uniformly sample a convex body [14]. As the set of all feasible activations is

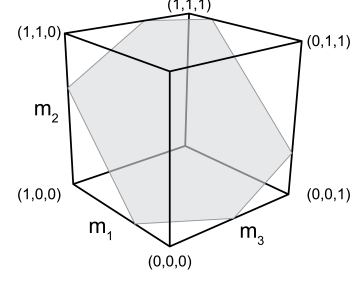


Fig. 1. The feasible activation set for a three-muscle system meeting one functional constraint is a polygon in \mathbb{R}^3 . Note that muscle activations are assumed to be bounded between 0 and 1.

defined by the mechanics of the limb and the constraints of the task (described in II-E), we decided to use Hit-and-run to sample muscle activation solutions from the polytope P . We refer to each sample from P as a 'point' $p \in [0, 1]^n$.

The Hit-and-Run walk on P is defined as follows (it works analogously for any convex body):

- 1) Find a starting point \mathbf{p} of P (Figure 2a) .
- 2) Generate a random direction from \mathbf{p} (uniformly at random over all directions) (Figure 2b).
- 3) Find the intersection points of the random direction with the edges of the polytope (Figure 2c).
- 4) Pick a random distance along the line formed by the endpoints (Figure 2d).
- 5) Repeat from (a) the above steps with the new point as the starting point .

B. Selecting a central seed point

To find a starting point in

$$\mathbf{f} = \mathbf{A}\mathbf{a}, \mathbf{a} \in [0, 1]^n,$$

we only need to find a feasible activation vector; that said, for the Hit-and-Run algorithm to mix faster we want a centrally located point within the polytope— that way, the early points will not be clustered in a corner [maytodo cite]. We use the following standard trick with slack variables ϵ_i to select a point where activations a_i for all muscles are far from 0 and 1, thereby finding a solution central within P [maytodo cite the use of slack variables to improve mixing time].

$$\begin{aligned} & \text{maximize} && \sum_{i=1}^n \epsilon_i \\ & \text{subject to} && \mathbf{f} = \mathbf{A}\mathbf{a} \\ & && a_i \in [\epsilon_i, 1 - \epsilon_i], \quad \forall i \in \{1, \dots, n\} \\ & && \epsilon_i \geq 0, \quad \forall i \in \{1, \dots, n\}. \end{aligned} \quad (1)$$

C. Removing inter-point dependence

As the function is recursive, any two successive points are not independent; therefore, we sample from our walk on P by selecting every m^{th} point to extract points which are distributed uniformly-at-random across P , and are independent to eachother. Some have said that it takes X

Hit-and-Run steps before the first and last points gathered are independent of one another, so we chose to collect every [maytodo confirm 100th] point into an array of points $M = [p_0, p_1, p_2, \dots, p_{100,000}]$.

D. Determining target sample size

How many points do we need to record from Hit-and-Run to reach a representative distribution across the polytope? For convex polygons in higher dimensions c. 40, experimental results suggest that $\mathcal{O}(n)$ steps of the Hit-and-Run algorithm are sufficient. In particular Emiris and Fisikopoulos paper suggest that $(10 + 10^{\frac{n}{2}})n$ steps are enough to converge upon the uniform distribution [6]. With the index finger model we collected a sample of [briantodo] points.

E. Realistic index finger model

We used our published model in [18] to find matrix $A \in \mathbb{R}^{4 \times 7}$, where $\mathbf{a} \in \mathbb{R}^7$; the four degrees of freedom were ad-abduction, flexion-extension at the metacarpophalangeal joint, and flexion-extension at the proximal and distal interphalangeal joints. The force directions we simulated are visible in Figure 3.

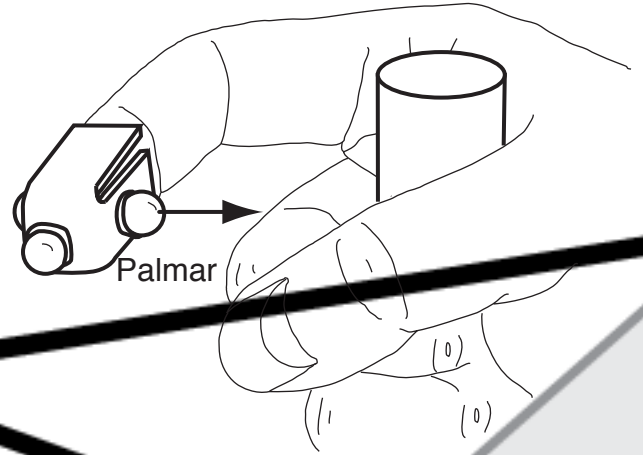
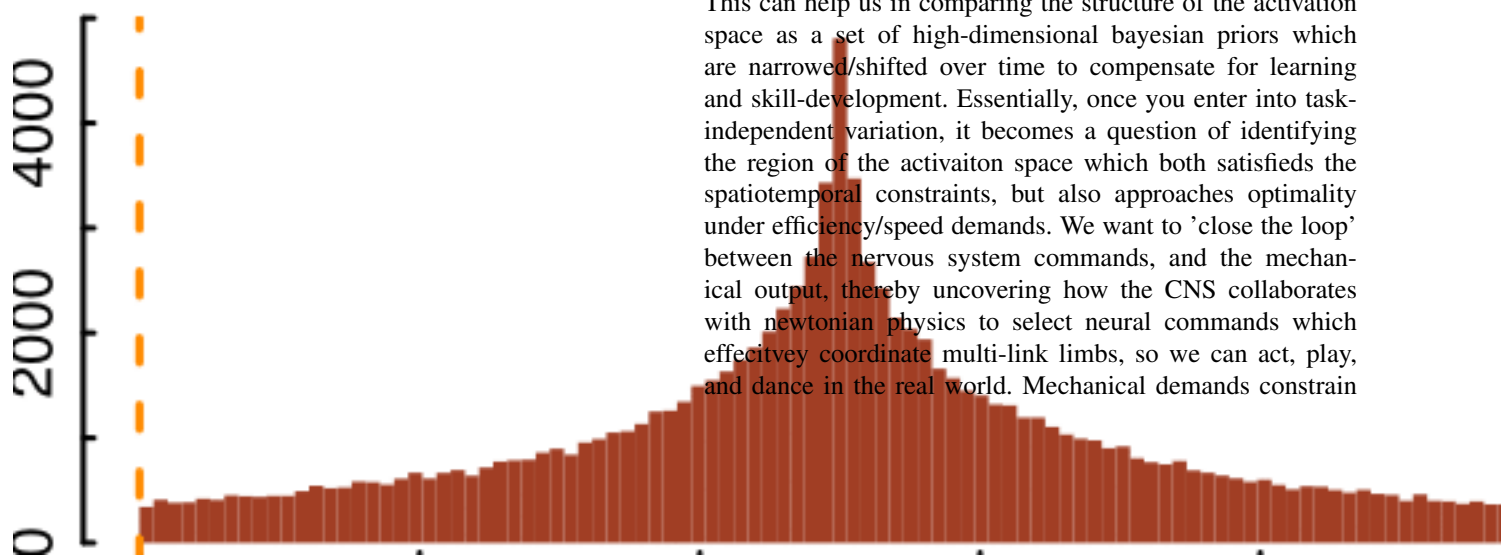
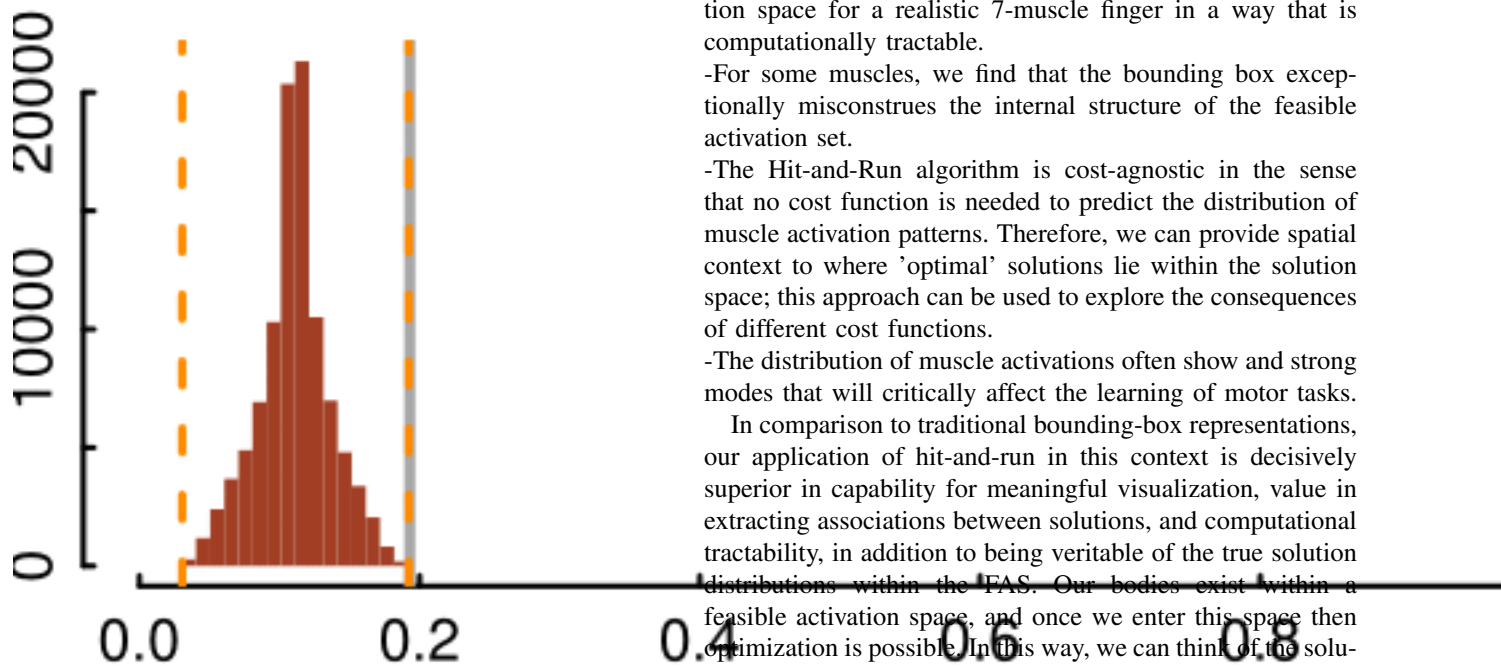
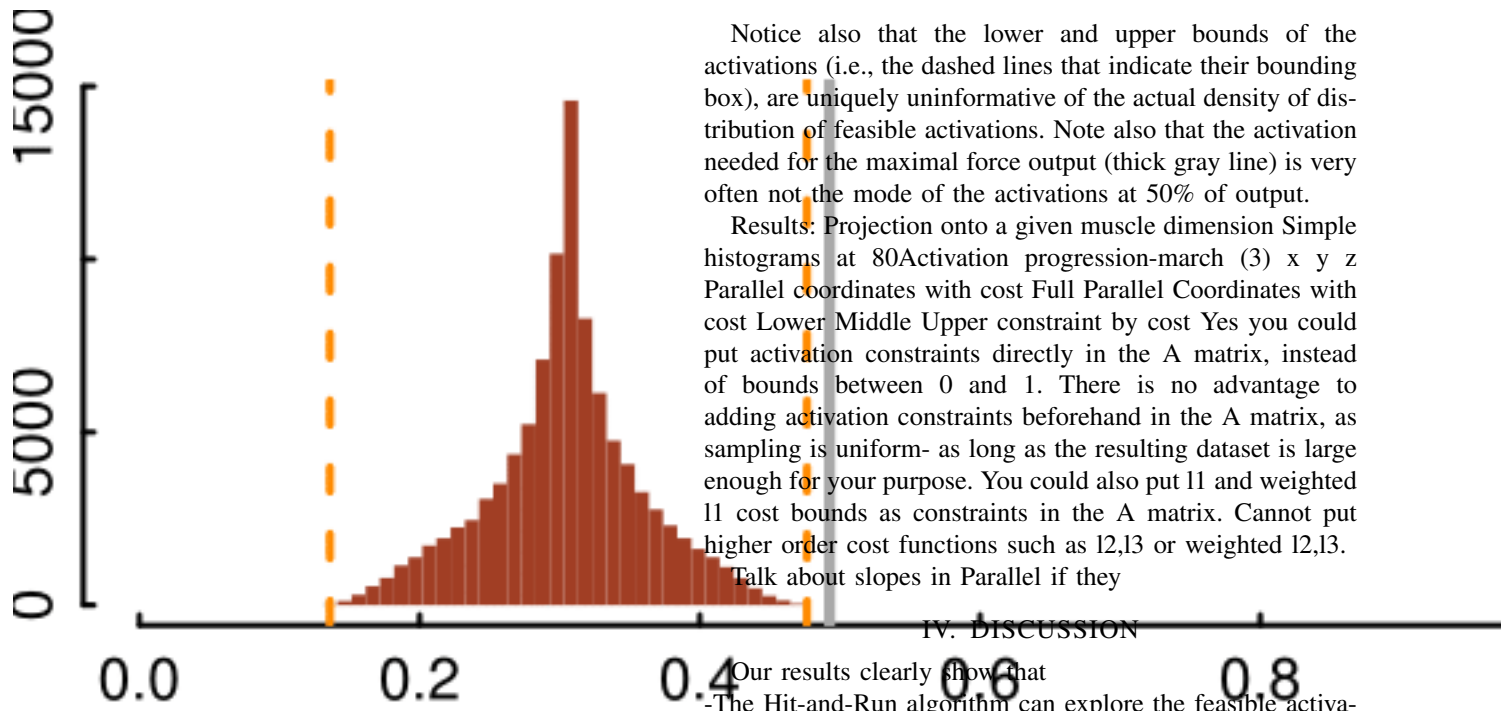


Fig. 3. The index finger model simulated 50% of maximal force production in the palmar direction. Adapted from [18].

We developed and tested our code on Ubuntu 14.04, Windows 8.1, and OSX Yosemite, using SciPy 2.11.6 [briantodo cite] for our implementation of Hit-and-Run, Matplotlib 3.1.3 [briantodo cite] for histograms and plots, and using Sygmatic Parcoord[briantodo cite] and d3.js[briantodo cite] for our interactive parallel coordinate visualization. All code required to replicate our research is readily available at <https://github.com/bcohn12/space>.

III. RESULTS

Using Hit-and-Run to sample feasible activation sets, Figure 4 shows the distributions of activation solutions for a palmar submaximal force. resulting from 1,000,000 solutions computed with Hit-and-Run sampling. This is the first time (to our knowledge) that the internal structure of the feasible activation set has been visualized for a sub-maximal force.



the total space of musculoskeletal coordination options, thus, motile organisms first 'explore' coordination strategies conducive to the desired movement, and recursively redefine the more optimal subspaces. Once a desired task is mapped to an effective coordination strategy (as in, it gets the job done), then training and experience (exploration-exploitation) can aid in finding the best coordination. As many tasks are similar (ie. they require the similar force generation or torque production over the course of a movement), the activation patterns for similar actions must be similar as well. Optimal coordination strategies for one task may be near-optimal for a similar task. On the other hand, a suboptimal coordination strategy that achieves one task, may be furiously off-target for a very similar task.

REFERENCES

- [1] D. Avis and K. Fukuda. A pivoting algorithm for convex hulls and vertex enumeration of arrangements and polyhedra. *Discrete & Computational Geometry*, 8(3):295–313, 1992.
- [2] E Y Chao and K N An. Graphical interpretation of the solution to the redundant problem in biomechanics. *Journal of Biomechanical Engineering*, 100:159–67, 1978.
- [3] R. H. Clewley, J. M. Guckenheimer, and F. J. Valero-Cuevas. Estimating effective degrees of freedom in motor systems. *IEEE Trans Biomed Eng*, 55:430–442, Feb 2008.
- [4] R.D. Crowninshield and R.A. Brand. A physiologically based criterion of muscle force prediction in locomotion. *Journal of Biomechanics*, 14(11):793–801, 1981.
- [5] Andrea d'Avella and Emilio Bizzi. Shared and specific muscle synergies in natural motor behaviors. *Proceedings of the National Academy of Sciences of the United States of America*, 102(8):3076–3081, 2005.
- [6] Ioannis Z Emiris and Vissarion Fisikopoulos. Efficient random-walk methods for approximating polytope volume. *arXiv preprint arXiv:1312.2873*, 2013.
- [7] JS Higginson, RR Neptune, and FC Anderson. Simulated parallel annealing within a neighborhood for optimization of biomechanical systems. *Journal of biomechanics*, 38(9):1938–1942, 2005.
- [8] Valero-Cuevas F. J., Cohn B. A., Yngvason H. F., and Lawrence E. L. Exploring the high-dimensional structure of muscle redundancy via subject-specific and generic musculoskeletal models. *J Biomech*, In press, 2015.
- [9] Vijaya Krishnamoorthy, Simon Goodman, Vladimir Zatsiorsky, and Mark L Latash. Muscle synergies during shifts of the center of pressure by standing persons: identification of muscle modes. *Biological cybernetics*, 89(2):152–161, 2003.
- [10] Jason J Kutch and Francisco J Valero-Cuevas. Muscle redundancy does not imply robustness to muscle dysfunction. *Journal of biomechanics*, 44(7):1264–1270, 2011.
- [11] Jason J Kutch and Francisco J Valero-Cuevas. Challenges and new approaches to proving the existence of muscle synergies of neural origin. *PLoS computational biology*, 8(5):e1002434, 2012.
- [12] B. I. Prilutsky. Muscle coordination: the discussion continues. *Motor Control*, 4(1):97–116, 2000. 0 1087-1640 Journal article.
- [13] Stephen H Scott. Optimal feedback control and the neural basis of volitional motor control. *Nature Reviews Neuroscience*, 5(7):532–546, 2004.
- [14] Robert L Smith. Efficient monte carlo procedures for generating points uniformly distributed over bounded regions. *Operations Research*, 32(6):1296–1308, 1984.
- [15] M Hongchul Sohn, J Lucas McKay, and Lena H Ting. Defining feasible bounds on muscle activation in a redundant biomechanical task: practical implications of redundancy. *Journal of biomechanics*, 46(7):1363–1368, 2013.
- [16] Emanuel Todorov and Michael I Jordan. Optimal feedback control as a theory of motor coordination. *Nature neuroscience*, 5(11):1226–1235, 2002.
- [17] F. J. Valero-Cuevas. A mathematical approach to the mechanical capabilities of limbs and fingers. *Adv. Exp. Med. Biol.*, 629:619–633, 2009.
- [18] F. J. Valero-Cuevas, F. E. Zajac, and C. G. Bugar. Large index-fingertip forces are produced by subject-independent patterns of muscle excitation. *J Biomech*, 31:693–703, Aug 1998.